Springer

KSME

Journal of Mechanical Science and Technology 33 (1) (2019) 139~147
www.springerlink.com/content/1738-494x(Print)/1976-3824(Online)
DOI 10.1007/s12206-018-1214-5

A fractional approach to the time-temperature dependence of dynamic viscoelastic behavior †

Z. L. Li[1], Y. Qin[1], B. Sun[2], C. L. Jia[1], W. J. Zhang[1], B. J. Yan[1] and Q. L. Shi[1,*]

[1]*School of Mechanical Engineering, Taiyuan University of Science and Technology, Taiyuan 030024, China*
[2]*School of Applied Science, Taiyuan University of Science and Technology, Taiyuan 030024, China*

(Manuscript Received April 3, 2018; Revised September 1, 2018; Accepted September 6, 2018)

Abstract

Fractional derivative and WLF equation are effective in describing the dynamic behavior and time-temperature effect of viscoelastic damping materials, respectively. These approaches have essentially evolved from the viscoelastic constitutive behavior. Based on such intrinsic relation, a fractional time-temperature superposition principle model (FTTSPM) that integrates the fractional constitutive relation and WLF equation was proposed. The parameters of this model were determined by performing tensile and DMA tests, and the master curves at 5 °C constructed by FTTSPM and WLF equation were compared. The theoretical prediction over the extended frequency span as the master curves was made by using the fractional standard linear solid model (FSLSM) to validate FTTSPM. The numerical results show that FTTSPM conforms to the time-temperature superposition principle. The parameters α and B' in this model denote the impact of the material and environment on the shifted factor, respectively. For the storage and loss modulus, the extended frequency obtained by FTTSPM is broader than that obtained by the WLF equation. Moreover, the evaluation of the storage and loss modulus by FTTSPM is much closer to the theoretical prediction compared with that by the WLF equation. Therefore, FTTSPM is a concise and experiment-based approach with a higher precision and greater frequency-extended capacity compared with the WLF equation. However, FTTSPM inevitably faces a vertical shift when non-thermo-rheologically simple materials are considered. The physical mechanism and practical application of FTTSPM will be examined in further research.

Keywords: Dynamic behavior; Fractional model; Master curve; Time-temperature dependence; Viscoelastic modulus

1. Introduction

Viscoelastic damping materials have been used in many fields, such as automobile, building, and military equipment manufacturing, to passively control noise and vibration [1-4]. These materials convert noise and vibration energy into thermal energy, which is subsequently dissipated as a result of the hysteretic effect of the viscoelastic damping material.

The mechanical characteristics of viscoelastic damping materials are highly dependent on ambient temperature and frequency. The constants for these two factors are applied in the traditional analysis and design of viscoelastic damping structures, thereby producing results with poor accuracy [5]. To overcome this problem, the time-temperature superposition principle (TTSP) was developed, according to which the frequency spectra at various temperatures can be collapsed onto a master curve at the reference temperature by multiplying the shifted factors [6]. The master curve covers a wide reduced frequency range up to many orders of magnitudes. The shifted factor is an important variable for TTSP, and researchers [7] have accordingly developed many models for this factor. The Arrhenius and WLF equations are popular models that differentiate from applicable temperature ranges. In common noise and vibration control engineering, the viscoelastic structure is always used within the applicable temperature scope of the WLF equation, thereby making this equation the most widely used model for TTSP. Recent studies that employ the WLF equation have focused on parameter identification, model application, and extension [8]. Meanwhile, some studies have begun to examine the use of this equation in predicting the properties of newly developed materials [9]. Paulo et al. [10] employed TTSP to study the rheological behavior of rubber tires at a constant shear rate and obtained coherent experimental results. Lin et al. [11] established the relationship between the viscosity of the reversible phase and the temperature for segmented polyurethanes by using the WLF equation. Jacek et al. [12] discussed the dependence of WLF parameters on the strength of cohesive molecular interactions and the degree of chain stiffness at the microscopic molecular level. Schaffner et al. [13] extended the application of the WLF equation to pre-

*Corresponding author. Tel.: +86 18636979318, Fax.: +86 3496998115
E-mail address: shiqinglukj@163.com
† Recommended by Associate Editor Sungsoo Na

dict lag time with temperature dependence for three psychrotrophic bacteria. Deng et al. [14] investigated the viscoelastic damage characteristics of asphalt by using the WLF equation to expand the experimental frequency range up to several orders of magnitudes. Zhu et al. [15] predicted the rheological behavior of wheat gluten dough by using the WLF equation and provided a theoretical reference for manufacturing this dough. Liu et al. [16] experimentally investigated several automobile-used PVB films and obtained their WLF parameters by fitting the experimental data. Zhang et al. [5] established a mirror-image relation between the frequency and temperature spectra of viscoelastic materials based on TTSP and derived a six-parameter fractional model for the temperature spectrum.

Over the past few years, fractional derivative has been extensively incorporated into rheological models of viscoelastic materials because of its global correlation [17]. Fractional models are more capable of fitting the experimental data compared with integer models. Tang et al. [18] proposed a five-parameter fractional constitutive model for a rubber vibration absorber and deduced a parameter determination technique by transferring this model to the frequency domain. Li et al. [19] established a factional viscoelastic oscillator while considering the geometric factor and then applied this oscillator in the dynamic analysis of the viscoelastic suspension of a crawler vehicle. Hu et al. [20] studied the derivations of a fractional Maxwell model to fit the experimental data from Jimenez et al. [21] and achieved a high consistency for the amended parameters. Wharmby et al. [22] proposed a modified Maxwell model based on the fractional derivative theorem and derived its frequency response function via the inverse Laplace transform. Cao et al. [23] performed a time domain analysis of the fractional-order-weighted distributed parameter Maxwell model. Hwang et al. [24] developed a fractional derivative Kelvin model that considers the ambient temperature effect on HDR bearings. Zhu et al. [25] implemented a nonlinear fractional viscoelastic model for rail pads by treating the vehicle as a 10-DOF system and the slab track as a 3-layer Bernoulli-Euler beam.

As can be seen in the above literature review, both the WLF equation and fractional derivative are effective in characterizing TTSP and the rheological behavior of viscoelastic materials, respectively. These approaches are uniform at the constitutive level. However, to the best of the authors' knowledge, very few models have merged these two methods. This paper aims to fill such gap by deriving the fractional TTSP model (FTTSPM) based on the fractional viscoelastic constitutive relation and the WLF equation and by contrastively analyzing the characteristics of its parameters. The fractional standard linear solid model (FSLSM) is then employed to validate the FTTSPM.

2. Theoretical model

2.1 Brief summary of TTSP

The TTSP reveals the interrelation between the time-dependence and temperature-dependence of the rheological behavior of viscoelastic damping materials. The frequency spectra at different temperatures can be superposed by using the frequency-shifted factors according to this model (see Fig. 1), which allows the construction of a master curve that covers a wide frequency range at a reference temperature. A nomogram that denotes the total dynamic viscoelastic behaviors in a single plot can also be constructed by using TTSP. This nomogram is often used along with the master curve to predict broadband viscoelastic behaviors and to overcome the restrictions of current rheometers, which result from the limitations of newly developed vibration exciters adopting piezoelectric actuators that can only reach up to 3.5 kHz, which is far below several orders of magnitudes [26]. The transition relation of the frequency spectra at temperature T to reference temperature T_r is expressed as

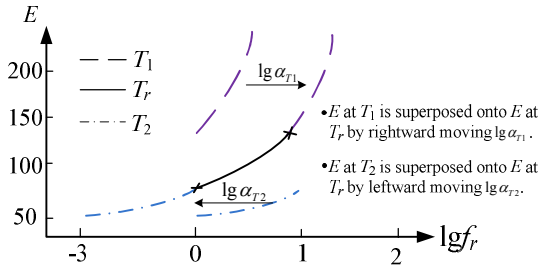

Fig. 1. Schematic graph of TTSP.

$$E(f,T) = E(f_r / \alpha_T, T_r), \tag{1}$$

where E represents the dynamic behaviors, such as storage modulus E', loss modulus E'', and loss factor (or loss tangent) η, f is the excitation frequency, f_r is the reduced frequency, and α_T is the frequency shifted factor. From Eq. (1), determining α_T plays an important role in the transition. Many TTSP models have been developed to address this problem, including the WLF equation, which was named after its proposers, William, Landel, and Ferry [27]. The original form of this equation is

$$\log \alpha_T = \frac{-C_1(T - T_r)}{C_2 + (T - T_r)}, \tag{2}$$

where C_1 and C_2 are constants depending on the material and the reference temperature. The logarithmic α_T directly indicates the horizontal shift of the isothermal at T when superposing into the isothermal at T_r.

2.2 Fractional TTSP model

Viscoelastic damping materials demonstrate both elastic and viscous behaviors and do not follow either Hooker's law or Newton's liquid rule. The fact that stress is proportional to the zero-order derivative of the strain in Hooker's law for pure elasticity and to the first-order derivative of the strain in New-

ton's liquid rule for pure viscosity inspires the fractional constitutive relationship for viscoelasticity, which takes the following form:

$$\sigma(t)=\gamma D^{\alpha}\varepsilon(t), \tag{3}$$

where σ and ε denote stress and strain, respectively, γ is the viscous coefficient, $\alpha(0<\alpha<1)$ is the derivative order, and $D^{\alpha}(\cdot)$ denotes the fractional derivative operator, whose Riemann–Liouville definition takes the following form:

$$D^{\alpha}\varepsilon(t)=\frac{1}{\Gamma(1-\alpha)}\frac{\mathrm{d}}{\mathrm{d}t}\int_0^t\frac{\varepsilon(\tau)}{(t-\tau)^{\alpha}}d\tau. \tag{4}$$

Executing the Laplace transform on Eq. (3) generates the following:

$$\bar{\sigma}=\gamma(\mathrm{i}\omega)^{\alpha}\bar{\varepsilon}, \tag{5}$$

where $\bar{\sigma}$ and $\bar{\varepsilon}$ are the Laplace transforms of σ and ε, respectively, $\omega=2\pi f$ is the angle frequency, and $\sqrt{-1}=\mathrm{i}$. The complex modulus E^*, which is defined as the ratio of $\bar{\sigma}$ to $\bar{\varepsilon}$, is given by

$$E^*=\frac{\bar{\sigma}}{\bar{\varepsilon}}=\gamma(\mathrm{i}\omega)^{\alpha} \tag{6}$$

and can be written as

$$\left|E^*\right|=\gamma\omega^{\alpha}. \tag{7}$$

Meanwhile, the viscous coefficient holds

$$\eta=\frac{\left|E^*\right|}{\omega^{\alpha}}. \tag{8}$$

To interpret the viscosity η as a temperature-dependent equilibrium, the following Vogel–Fulcher–Tammann equation in the free-volume system is employed:

$$\eta=\kappa\exp\frac{B}{T-T_0}, \tag{9}$$

where κ is the correction factor, B is the material factor, and T_0 is the critical temperature.

Given its dependence on temperature and frequency, E^* can be written as the function of T and ω, that is, $E^*(\omega,T)$. Equilibrating Eqs. (8) and (9) for (ω,T) and (ω_r,T_r) leads to

$$\frac{\left|E^*(\omega,T)\right|}{\omega^{\alpha}}=\kappa\exp\frac{B}{T-T_0} \tag{10a}$$

$$\frac{\left|E^*(\omega_r,T_r)\right|}{\omega_r^{\alpha}}=\kappa\exp\frac{B}{T_r-T_0}. \tag{10b}$$

Taking the logarithm operation on both ends of Eqs. (10a) and (10b) and then subtracting the second one from the first one will yield

$$\begin{aligned}&\ln\left|E^*(\omega,T)\right|-\ln\left|E^*(\omega_r,T_r)\right|-\ln\omega^{\alpha}+\ln\omega_r^{\alpha}\\&=\frac{B(T_r-T)}{(T-T_0)(T_r-T_0)}\end{aligned}. \tag{11}$$

By taking into account TTSP, we have $E^*(\omega,T)=E^*(\omega_r,T_r)$. Therefore, Eq. (11) is rewritten as

$$\ln\left(\frac{\omega_r}{\omega}\right)^{\alpha}=\frac{B(T_r-T)}{(T_r-T_0)(T-T_0)}. \tag{12}$$

Eq. (12) is the primary form of FTTSPM that reveals the mathematical relationship of dynamic viscoelastic behaviors at (ω,T) and (ω_r,T_r).

A variant of the WLF equation is $\log\alpha_T=-C_1\Delta T/(C_2+\Delta T)$, where $\Delta T=T-T_r$. The shifted factor α_T is only dependent on ΔT within the temperature scope of the WLF equation. Therefore, we assume that the shifted factor from FTTSPM merely responds to ΔT as the WLF equation, that is,

$$\ln\left(\frac{\omega_r}{\omega}\right)^{\alpha}=\frac{-B\Delta T}{(T_r-T_0)(T-T_0)}. \tag{13}$$

The term $(T-T_0)(T_r-T_0)$ on the righthand side of Eq. (13) is constant due to the single-variable hypothesis for α_T of FTTSPM, that is, $(T-T_0)(T_r-T_0)=T_{cons}$. Therefore, Eq. (13) can be shortened as

$$\ln\left(\frac{\omega_r}{\omega}\right)^{\alpha}=-B'\Delta T, \tag{14}$$

where $B'=B/T_{cons}$ is constant. Here, the frequency shifted factor by FTTSPM takes the form

$$\alpha_T=\sqrt[\alpha]{\frac{1}{\mathrm{e}^{B'\Delta T}}}. \tag{15}$$

The α_T determined by Eq. (15) contains two parameters, namely, α and B', which reflect the material and environment influences on TTSP, respectively. Therefore, these parameters are designated as the material parameter and environment parameter, respectively. The parameters of FTTSPM are determined as follows.

Step 1. The value of material parameter α is obtained by fitting Eq. (3) against the strain–stress curve obtained by the

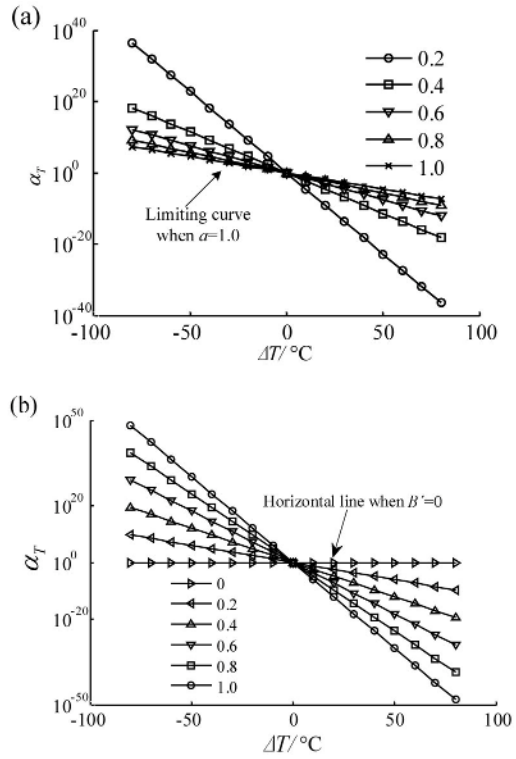

Fig. 2. Parameter dependence of α_T: (a) α = 0.2, 0.4, 0.6, 0.8, 1.0 and B' = 0.2; (b) B' = 0, 0.2, 0.4, 0.6, 0.8, 1.0 and α = 0.8.

tensile test on the standard sample.

Step 2. The temperature spectra of the dynamic viscoelastic behavior at n frequencies are obtained by performing the DMA test. For the temperature spectra of a certain dynamic behavior, a horizontal line that intersects the ω_i-spectrum at (ω_i, T_i) i = 1, 2, … n is drawn. At this time, the environment parameter B' is obtained by fitting Eq. (14) against (ω_i, T_i) i = 1, 2, … n.

2.3 Parameter analysis

To understand the parameter influence on the α_T of FTTSPM, the variations in α_T along with ΔT are numerically studied across different magnitudes of α and B'. Typical results with parameters of α = 0.2, 0.4, 0.6, 0.8, 1 and B' = 0, 0.4, 0.6, 0.8, 1 are shown in Figs. 2(a) and (b).

Figs. 2(a) and (b) reveal that α_T is a monotonically decreasing function of ΔT. lgα_T is positive when $T < T_r$, thereby suggesting that the isothermal at T is horizontally superposed right onto the higher frequency region of the master curve at T_r. However, lgα_T is negative when $T > T_r$, thereby indicating that the isothermal at T is horizontally superposed left onto the lower frequency region of the master curve at T_r.

Fig. 2(a) also shows that α_T decreases when $\Delta T < 0$ °C and $\Delta T > 0$ °C increase along with α for a specific temperature. These trends indicate that the horizontal superposition of the unit temperature variation is smaller for a greater viscosity (larger magnitude of fractional order α). It is calculably found that $\alpha_T \to \infty$ for α = 0 because Eq. (3) degenerates into a complete Hooker's unit that does not follow the TTSP. Another extreme curve is observed when α = 1 as indicated by the arrow in Fig. 2(a), thereby suggesting a purely viscous state.

For the environment parameter, Fig. 2(b) shows that α_T decreases when $\Delta T > 0$ °C and $\Delta T < 0$ °C increase along with B' for a specific temperature. The curve of α_T for B' = 0 is horizontal and equal to 1 as indicated by the arrow in Fig. 2(b). No horizontal shift occurs under this condition because the molecular of the viscoelastic damping material remains in a frozen state.

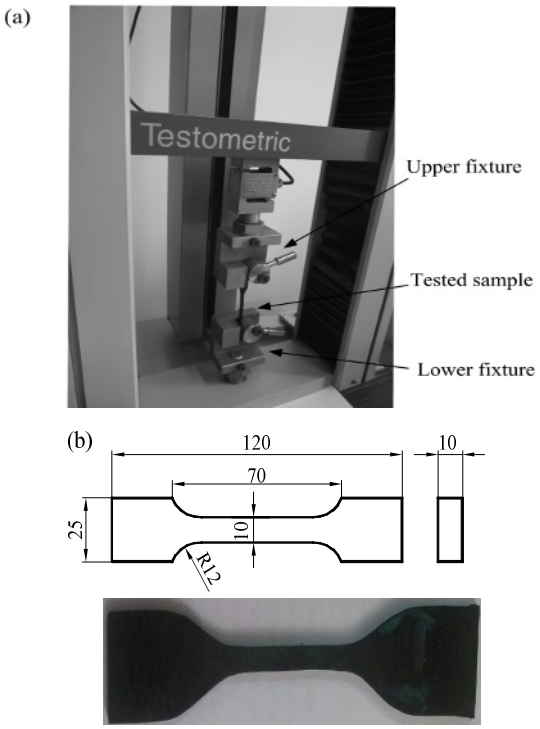

Fig. 3. Tensile test: (a) Apparatus; (b) elongation sample.

3. Experiment

The viscoelastic damping material used in controlling the vibration of engineering vehicles is selected as the study case. This viscoelastic damping material is made from sulphur-cured natural rubber with a specific ratio of some agents (accelerator, antiager, filler, etc.) by a special process. Given its excellent damping performance for low-frequency and heavy alternating loads, this material has been successfully applied in the viscoelastic suspension of crawler vehicles, roadheaders, and others.

3.1 Tensile test

Tensile test is conducted following ISO 37:2011 on the I-dumbbell sample by using an M350-10 kN-type precise elongation apparatus (Testometric, Britain) as shown in Figs. 3(a) and (b).

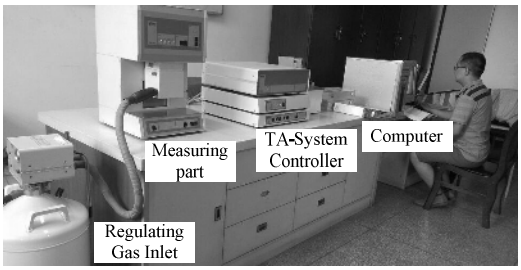

Fig. 4. DMA 242C set up.

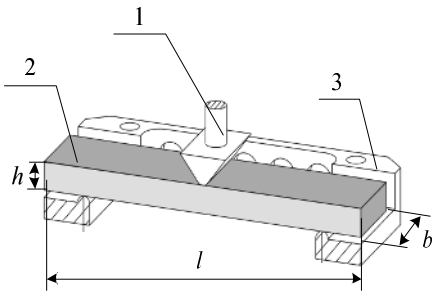

Fig. 5. Three-point bending mode: 1—Push rod; 2—Sample; 3—Sample holder.

3.2 DMA test

The DMA (dynamic thermal analytical method) test is widely used for measuring the dynamic mechanical response of viscoelastic damping materials subjected to a specific temperature-frequency program [28]. The DMA test in this study is performed according to ISO 6721-1 on DMA 242C (Netzsch, Germany, Fig. 4). The three-point bending mode is selected, in which the sample is supported on two supporting edges, while the probe edge applies the load to the sample as shown in Fig. 5. The sample is excited by loads of 0.5, 1, 2, 3.33, 5 and 10 Hz over a temperature range of –120 °C to 120 °C at intervals of 2 °C/min. A static force larger than the dynamic force must be applied on the sample to prevent it from jumping off the holder. The atmosphere in the sample chamber is maintained by nitrogen. The temperature is sensed by the thermocouple placed close to the sample (approximately 1 mm) and adjusted automatically by the controller. The complex modulus of the sample can be derived by

$$E^* = \frac{l^3}{4bh^3}\frac{F}{d}, \tag{16}$$

where l, h and b denote the depth, width, and height of the sample, respectively, F denotes the exciting force, and d denotes the displacement. After obtaining the complex modulus, the other dynamic behaviors, including the storage modulus E', loss modulus E'', and loss factor η, can be obtained by the corresponding transformation. The computation processes are automatically completed by the DMA software based on logged data. The temperature spectra obtained from the DMA test are presented in Fig. 6.

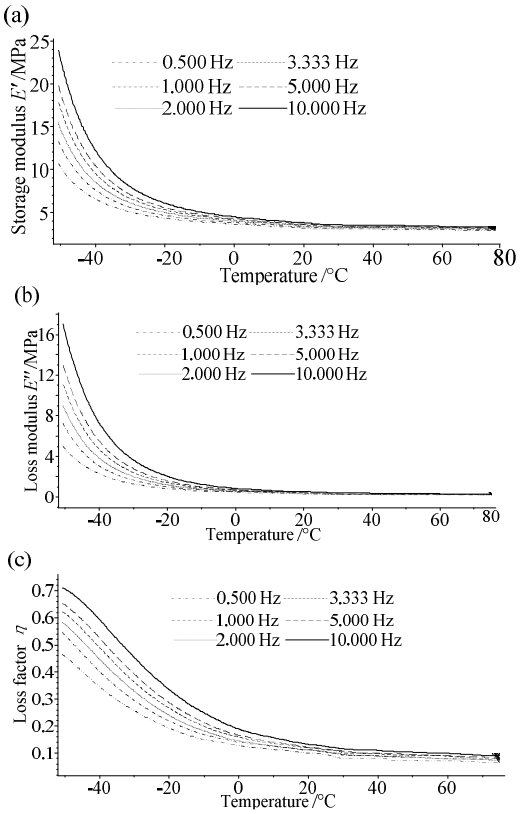

Fig. 6. (a) Temperature spectra of storage modulus E'; (b) loss modulus E''; (c) loss factor η.

The DMA test reveals that the dynamic behaviors of the viscoelastic material are dependent on temperature and frequency. The storage modulus E', loss modulus E'', and loss factor η monotonically decrease within the considered temperature and tend to be flat over 60 °C due to the thermal softening effect. Therefore, effective heat-dissipating measures must be adopted in engineering practice to ensure a sufficient modulus and to avoid thermally induced defects. A positive correlation can also be observed between the spectra and the frequency for a specific temperature. This correlation weakens as the temperature increases. As will be discussed in the next section, the master curve can help reveal the comprehensive dependence of dynamic behaviors on temperature and frequency.

4. Comparison and validation

For comparison and validation purposes, the master curves of the dynamic behaviors of the viscoelastic material are constructed by using the WLF equation and FTTSPM and are validated by using FSLSM.

4.1 Parameter determination

Following Step 1 of the parameter determination procedure of FTTSPM, the material parameter α is determined as 0.7410 by fitting Eq. (3) against the strain–stress data derived from

Table 1. Fitting data groups for B' in FTTSPM.

Frequency/Hz		0.5	1	2
Temperature/°C	for E'	-76.0	-73.7	-71.2
	for E''	-70.4	-67.0	-64.4
	for η	-56.9	-47.3	-43.9
Frequency/Hz		3.33	5	10
Temperature/°C	for E'	-69.4	-68	-65.9
	for E''	-62.4	-61.0	-57.8
	for η	-40.7	-38.2	-33.4

Table 2. Parameters of the WLF equation.

Parameter	For storage modulus	For loss modulus	For loss factor
C_1	90.5	90.5	58.3
C_2/K	788.5	1024.5	899.0

the tensile test.

For environment parameter B', the data are fitted against ω_i, T_i following step 2 of the parameter determination procedure. The fitting data groups are listed in Table 1. By taking the data in the third column of Table 1 as reference (ω_r, T_r) and by fitting Eq. (14), E', E'' and η obtain B' magnitudes of 0.2103, 0.177 and 0.0900, respectively.

The parameters for the WLF equation are extracted by using the DMA software Proteus Analysis. The results are listed in Table 2.

4.2 Theoretical prediction

FSLSM is a five-parameter constitutive model of viscoelastic damping materials that is reasonably capable of describing real viscoelastic behavior at a broad frequency range [29]. This model can be mathematically expressed as

$$\sigma + bD^{\beta_1}\sigma = E_0\varepsilon + E_1 D^{\beta_2}\varepsilon\,, \tag{17}$$

where β_1 and β_2 are fractional orders, b, while E_0 and E_1 are material constants.

The complex modulus is derived by transforming Eq. (17) into the frequency domain

$$E^* = \frac{\bar{\sigma}}{\bar{\varepsilon}} = \frac{E_0 + E_1(\mathrm{i}\omega)^{\beta_2}}{1 + b(\mathrm{i}\omega)^{\beta_1}}\,, \tag{18}$$

where E^* denotes the complex modulus.

Applying mathematical manipulations on the real and imaginary parts of Eq. (18) yields the following components of the complex modulus:

$$E' = \frac{xy + E_1 b\omega^{(\beta_1+\beta_2)}\sin\frac{\beta_2}{2}\pi\sin\frac{\beta_1}{2}\pi}{y^2 + b^2\omega^{2\beta_1}\sin^2\frac{\beta_1}{2}\pi}\,, \tag{19}$$

$$E'' = \frac{yE_1\omega^{\beta_2}\sin\frac{\beta_2}{2}\pi - xb\omega^{\beta_1}\sin\frac{\beta_1}{2}\pi}{y^2 + b^2\omega^{2\beta_1}\sin^2\frac{\beta_1}{2}\pi}\,, \text{ and} \tag{20}$$

$$\eta = \frac{yE_1\omega^{\beta_2}\sin\frac{\beta_2}{2}\pi - xb\omega^{\beta_1}\sin\frac{\beta_1}{2}\pi}{xy + E_1 b\omega^{(\beta_1+\beta_2)}\sin\frac{\beta_2}{2}\pi\sin\frac{\beta_1}{2}\pi}\,, \tag{21}$$

where $x = E_0 + E_1\omega^{\beta_2}\cos\frac{\beta_2}{2}\pi$ and $y = 1 + b\omega^{\beta_1}\cos\frac{\beta_1}{2}\pi$.

We obtain the FSLSM parameters b = 0.45, β_1 = 0.15, β_2 = 0.7, E_0 = 1.95e6 and E_1 = 2.07e6 by fitting the frequency spectra of viscoelastic dynamic behaviors at 5 °C.

4.3 Results and discussion

The magnitudes of α_T of WLF and FTTSPM for different temperatures with respect to T_r = 5 °C are derived by using Eqs. (2) and (15) and are shown in Table 3. Given that a data fitting technology is adopted to deal with the test data, the magnitudes of α_T differ across the considered dynamic behaviors at the reference temperature. The master curves of storage modulus, loss modulus, and loss factor as obtained by FTTSPM and WLF are constructed. For comparison and validation purposes, the dynamic behaviors are predicted as master curves by FSLSM over the similar frequency ranges. The comparison curves are shown in Fig. 7.

Table 3 shows that the frequency ranges of the dynamic behaviors are broadly extended by TTSP and cover approximately 10 orders of magnitude. For the storage and loss modulus, the extended frequencies obtained by FTTSPM are broader than those obtained by WLF, especially at very low frequencies. However, the opposite effect is observed for the loss factor. lgα_T is positive for temperatures below T_r and negative for temperatures above T_r, thereby indicating that FTTSPM conforms to the hypothesis of TTSP.

Table 3 also shows that different shifted factors correspond to different dynamic parameters at a given reference temperature. Such differences can be attributed to two reasons. On the one hand, the storage modulus and loss modulus are the real and imaginary parts of the complex modulus, respectively. The DMA test measures the exciting force and displacement of the sample, while the complex modulus is obtained by using Eq. (16). Afterward, the components of the complex modulus are obtained by applying some mathematical manipulations, which can introduce some errors and yield different "average relaxation times" for the storage modulus and loss modulus. On the other hand, the loss factor demonstrates an error accumulation effect because this factor is obtained via (loss modulus)/(storage modulus). The fitting process also contributes to the differences in the shifted factor because the fitting model itself is a phenomenological model.

Figs. 7(a) and (b) reveal that the storage modulus and loss modulus increase along with the reduced frequency at T_r = 5 °C.

Table 3. Shifted factors for different temperatures at T_r = 5 °C.

Temperature/°C	lgα_T for storage modulus		lgα_T for loss modulus		lgα_T for loss factor	
	WLF	FTTSPM	WLF	FTTSPM	WLF	FTTSPM
-75	10.2175	10.1430	7.6654	8.2648	5.7651	4.1716
-65	8.8169	8.8756	6.6370	7.2324	4.9829	3.6502
-55	7.4537	7.6078	5.6299	6.1992	4.2195	3.1287
-45	6.1273	6.3399	4.6434	5.1660	3.4744	2.6073
-35	4.8363	5.0719	3.6770	4.1328	2.7468	2.0858
-25	3.5794	3.8039	2.7300	3.0996	2.0361	1.5644
-15	2.3552	2.5360	1.8019	2.0664	1.3418	1.0429
-5	1.1625	1.2680	0.8921	1.0332	0.6633	0.5215
5	0.0000	0.0000	0.0000	0.0000	0.0000	0.0000
15	-1.1334	-1.2680	-0.8748	-1.0332	-0.6485	-0.5214
25	-2.2387	-2.5360	-1.7329	-2.0664	-1.2827	-1.0429
35	-3.3170	-3.8041	-2.5746	-3.0996	-1.9032	-1.5644
45	-4.3696	-5.0721	-3.4001	-4.1325	-2.5102	-2.0857
55	-5.3969	-6.3401	-4.2111	-5.1662	-3.1046	-2.6073
65	-6.3990	-7.6073	-5.0070	-6.1993	-3.6861	-3.1290
75	-7.3788	-8.8761	-5.7878	-7.2321	-4.2557	-3.6498

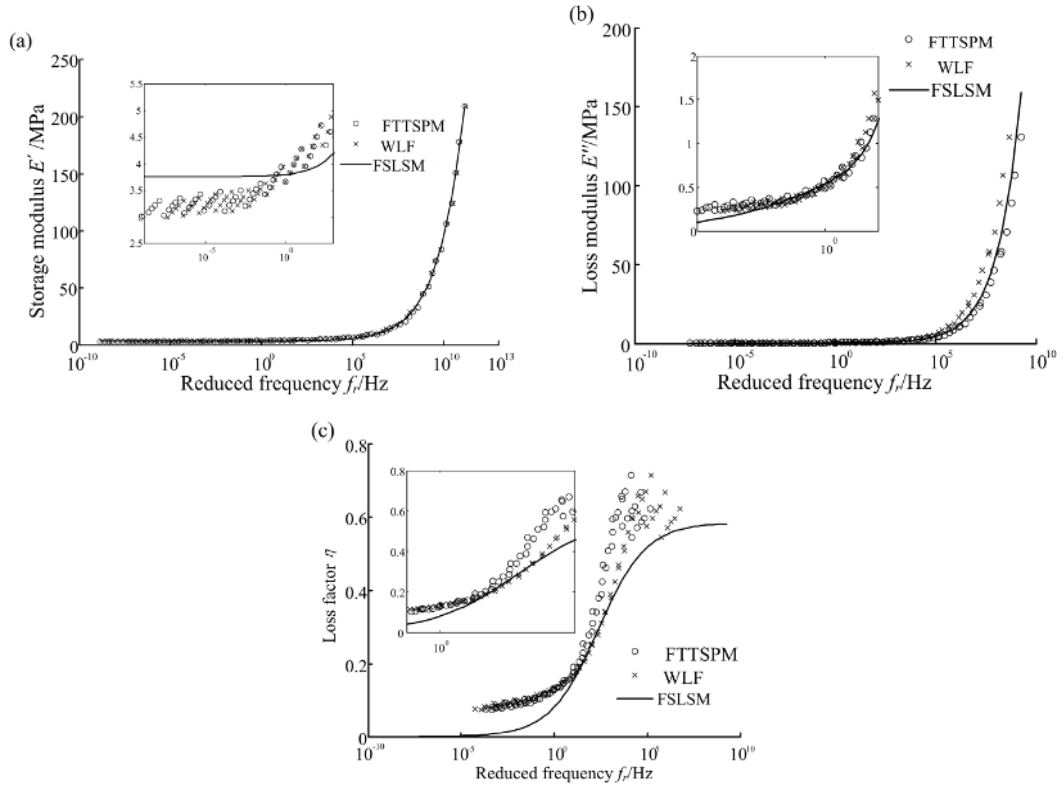

Fig. 7. Master curves for (a) storage modulus; (b) loss modulus; (c) loss factor as predicted by FTTSPM, WLF and FSLSM, respectively.

The master curves obtained by FTTSPM and WLF are consistent with the predictions of FSLSM. Compared with WLF, the data obtained by FTTSPM are much closer to the FSLSM curve. The subplot in Fig. 7(a) shows that the E' master curve at lower frequency is scattered, thereby suggesting that the isothermals at higher temperatures are poorly superposed onto the lower reduced frequency range. To interpret this result further, the Wicket-plot, where the loss factor is plotted versus the storage modulus, is presented in Fig. 8. The figure shows that the curves are dependent on temperature, thereby proving

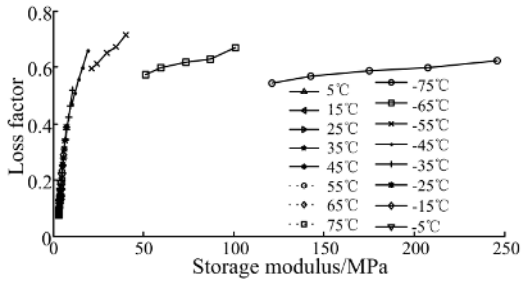

Fig. 8. Wicket-plot.

that the tested material is not thermo-rheologically simple. In this case, a vertical shift is inevitable when constructing a smooth master curve.

Fig. 7(c) shows that the η master curves are not well constructed by both FTTSPM and WLF and greatly deviate from the curve predicted by FSLSM, except in the experiment frequency range of 0 Hz to 10 Hz. This result can be explained further by the Wicket-plot in Fig. 8, which shows that the horizontal shift is not enough for this case. The actual errors also accumulate when evaluating the ratio of the loss modulus to the storage modulus in order to derive the loss factor. These errors also significantly contribute to the poor master curves of the loss factor.

5. Conclusions

The FTTSPM was developed by integrating the WLF equation into fractional viscoelasticity to describe the time-temperature dependence of viscoelastic behaviors. The parameter characteristics of FTTSPM were analyzed and compared with those of the WLF equation. The master curves of the viscoelastic modulus were constructed by using FTTSPM and were validated by using FSLSM. The following conclusions can be drawn from the findings of this work:

(1) FTTSPM conforms to the time-temperature superposition principle for $0 < \alpha < 1$. The shifted factor approaches infinity when $\alpha = 0$ because the fractional viscoelastic model degenerates into a complete Hooker's unit. Moreover, the situation in $\alpha = 1$ suggests a purely viscous state.

(2) The parameters α and B' of FTTSPM denote the impact of the material and environment on the shifted factor α_T, respectively, and can be experimentally determined. For the storage and loss modulus, the extended frequency obtained by FTTSPM is broader than that obtained by the WLF equation, especially at very low frequencies. This result highlights the high frequency-extended capacity of FTTSPM.

(3) Compared with those of the WLF equation, the results of FTTSPM for the evaluation of storage and loss modulus are much closer to those of FSLSM. However, the master curves for the loss factor are scattered and poorly fitted by FSLSM because of the serious temperature dependence of the material properties and the actual error accumulation from the storage and loss modulus.

(4) Future studies must examine the incorporation of the vertical shift into FTTSPM. The physical mechanism and application of FTTSPM for controlling noise and vibration in engineering practice must also be investigated.

Acknowledgments

This work was sponsored by the National Natural Science Foundation of China (51805347), the TYUST Foundation for Doctor (20162035), and the Fund for Shanxi "1331 Project" Key Subjects Construction (1331KSC).

Nomenclature

T	: Temperature
T_r	: Reference temperature
E	: Dynamic behavior
E^*	: Complex modulus
E'	: Storage modulus
E''	: Loss modulus
η	: Loss factor (or loss tangent)
f	: Excitation frequency
f_r	: Reduced frequency
α_T	: Frequency shifted factor
σ	: Stress
ε	: Strain
λ	: Viscous coefficient
$\alpha(0 < \alpha < 1)$	: Derivative order
$\overline{\sigma}$	: Laplace transform of σ
$\overline{\varepsilon}$	: Laplace transform of ε
κ	: Correction factor
B	: Material factor
T_0	: Critical temperature
B'	: Environment parameter
l	: Depth
h	: Width
b	: Height
F	: Exciting force
d	: Displacement
β_1, β_2	: Fractional orders

References

[1] W. Y. Jung and A. J. Aref, A combined honeycomb and solid viscoelastic material for structural damping applications, *Mechanics of Materials*, 35 (8) (2003) 831-844.

[2] C. H. Park, S. J. Ahn, H. C. Park and S. Na, Modeling of a hybrid passive damping system, *Journal of Mechanical Science and Technology*, 19 (1) (2005) 127-135.

[3] R. K. Singh, R. Kant, S. S. Pandey, M. Asfer, B. Bhattacharya, P. k. panigrahi and S. Bhattacharya, Passive vibration damping using polymer pads with microchannel arrays, *Journal of Microelectromechanical Systems*, 22 (3) (2013) 695-707.

[4] M. Mohammadimehr, A. A. Monajemi and M. Moradi, Vibration analysis of viscoelastic tapered micro-rod based on

strain gradient theory resting on visco-pasternak foundation using DQM, *Journal of Mechanical Science and Technology*, 29 (6) (2015) 2297-2305.

[5] Z. L. Zhang, S. Q. Li, and W. G. Zhu, Temperature spectrum model of dynamic mechanical properties for viscoelastic damping materials, *Journal of Mechanical Engineering*, 47 (20) (2011) 135.

[6] D. G. Fesko and N. W. Tschoegl, Time-temperature superposition in thermorheologically complex materials, *Journal of Polymer Science Polymer Symposia*, 35 (1) (2010) 51-69.

[7] P. Micha, On the use of the WLF model in polymer and foods, *Critical Reviews in Food Science and Nutrition*, 32 (1) (1992) 59-66.

[8] B. K. Ashokan and J. L. Kokini, Determination of the WLF constants of cooked soy flour and their dependence on the extent of cooking, *Rheologica Acta*, 45 (2) (2005) 192-201.

[9] A. Mathias, K. Ulrich and F. Petra, Evaluation of the relevance of the glassy state as stability criterion for freeze-dried bacteria by application of the Arrhenius and WLF model, *Cryobiology*, 65 (3) (2012) 308-318.

[10] P. Lima, S. Silva, J. Oliveira and V. Costa, Rheological properties of ground tyre rubber based thermoplasitc elastomeric blends, *Polymer Testing*, 45 (2015) 58-67.

[11] J. R. Lin and L. W. Chen, The mechanical-viscoelastic model and WLF relationship in shape memorized linear ether-type polyurethanes, *Journal of Polymer Research*, 6 (1) (1999) 35-44.

[12] J. Dudowicz, J. F. Douglas and K. F. Freed, The meaning of the "universal" WLF parameters of glass-forming polymer liquids, *The Journal of Chemical Physics*, 142 (1) (2015) 014905.

[13] D. W. Schaffner, The application of the WLF equation to predict lag time as a function of temperature for three psychrotrophic bacteria, *International Journal of Food Microbiology*, 27 (2-3) (1995) 107-115.

[14] J. L. Zheng, S T Lu and X. G. Tian, Viscoelastic damage characteristics of asphalt based on creep test, *Engineering Mechanics*, 25 (2008) 193-196.

[15] F. Zhu, G. W. Xu and W. P. Ding, Tube theory based analysis on the rheological behavior of wheat gluten dough, *Transactions of the Chinese Society of Agricultural Engineering*, 23 (7) (2007) 24-29.

[16] B. H. Liu, J. Zhou, Y. T. Sun, Y. Wang, J. Xu and Y. B. Li, An experimental study on the dynamic viscoelasticity of PVB film material for vehicle, *Automotive Engineering*, 34 (10) (2012) 898-904+927.

[17] M. R. Permoon, J. Rashidinia, A. Parsa, H. Haddadpour and R. Salehi, Application of radial basis functions and sinc method for solving the forced vibration of fractional viscoelastic beam, *Journal of Mechanical Science and Technology*, 30 (7) (2016) 3001-3008.

[18] Z. H. Tang, G. H. Luo, W. Chen and X. G. Yang, Dynamic characteristics of vibration system including rubber isolator, *Journal of Nanjing University of Aeronautics & Astronautics*, 46 (2) (2014) 285-291.

[19] Z. L. Li, D. G. Sun, B. Sun, B. J. Yan, B. H. Han and J. Meng, Fractional model of viscoelastic oscillator and application to a crawler tractor, *Noise Control Engineering Journal*, 64 (3) (2016) 388-402.

[20] K. X. Hu and K. Q. Zhu, A note on fractional Maxwell model for PMMA and PTFE, *Polymer Testing*, 30 (7) (2011) 797-799.

[21] A. Hernández-Jiménez, J. Hernández-Santiago, A. Macias-García and J. Sánchez-González, Relaxation modulus in PMMA and PTFE fitting by fractional Maxwell model, *Polymer Testing*, 21 (3) (2002) 325-331.

[22] A. W. Wharmby and R. L. Bagley, Modifying Maxwell's equations for dielectric materials based on techniques from viscoelasticity and concepts from fractional calculus, *International Journal of Engineering Science*, 79 (2014) 59-80.

[23] L. L. Cao, Y. Li, G. H. Tian, B. D. Liu and Y. Q. Chen, Time domain analysis of the fractional order weighted distributed parameter Maxwell model, *Computers & Mathematics with Applications*, 66 (5) (2013) 813-823.

[24] J. S. Hwang and T. Y. Hsu, A fractional derivative model to include effect of ambient temperature on HDR bearings, *Engineering Structures*, 23 (5) (2001) 484-490.

[25] S. Y. Zhu, C. B. Cai and P. D. Spanos, A nonlinear and fractional derivative viscoelastic model for rail pads in the dynamic analysis of coupled vehicle–slab track systems, *Journal of Sound and Vibration*, 335 (2015) 304-320.

[26] F. Renaud, G. Chevallier, J. L. Dion and R. Lemaire, Viscoelasticity measurements and identification of viscoelastic parametric models, *ASME 2011 International Design Engineering Technical Conferences and Computers and Information in Engineering Conference*, Washington, DC, USA (2011) 701-708.

[27] M. L. Williams, R. F. Landel and J. D. Ferry, The temperature dependence of relaxation mechanisms in amorphous polymers and other glass-forming liquids, *Journal of the American Chemical Society*, 77 (14) (1955) 3701-3707.

[28] P. Jindal, R. N. Yadav and N. Kumar, Dynamic mechanical characterization of PC/MWCNT composites under variable temperature conditions, *Iranian Polymer Journal*, 26 (6) (2017) 445-452.

[29] J. J. Espindola, M. S. Joao and M. O. Eduardo, A generalized fractional derivative approach to viscoelastic material properties measurement, *Applied Mathematics and Computation*, 164 (2) (2005) 493-506.

Li Zhanlong obtained his Ph.D. degree from Xi'an University of Technology and is currently serving as a lecturer at Taiyuan University of Science and Technology. His research interests include viscoelastic mechanics and its application in vibration and noise control.